Dyes and Pigments 95 (2012) 252–259

Contents lists available at SciVerse ScienceDirect

Dyes and Pigments

journal homepage: www.elsevier.com/locate/dyepig

Naphthoylenebenzimidazolone dyes as electron transfer photosensitizers for iodonium salt induced cationic photopolymerizations

Radosław Podsiadły [a,*], Anna Maruszewska [a], Radosław Michalski [b], Andrzej Marcinek [b], Jolanta Kolińska [a]

[a] Institute of Polymer and Dye Technology, Technical University of Lodz, Stefanowskiego 12/16, 90-924 Lodz, Poland
[b] Institute of Applied Radiation Chemistry, Technical University of Lodz, Zeromskiego 116, 90-924 Lodz, Poland

ARTICLE INFO

Article history:
Received 2 February 2012
Received in revised form
4 April 2012
Accepted 7 April 2012
Available online 23 April 2012

Keywords:
Photosensitizers
Radical cation
Naphthoylenebenzimidazolone dyes
Cationic photopolymerization
Photoinduced electron transfer
Photobleaching

ABSTRACT

Photoredox pairs, consisting of naphthoylenebenzimidazolone dyes and commercially available diphenyliodonium salts, are effective visible wavelength initiators for the cationic polymerization of cyclohexene oxide in air. The efficiencies of these initiator systems are based on the free energy change of the electron transfer from the naphthoylenebenzimidazolone dyes to the onium compounds. Experimental results show that the ability of tested photoredox pairs to initiate the photopolymerization strongly depends upon the oxidation potentials of the naphthoylenebenzimidazolone dyes and the reduction potentials of the iodonium salts. Additionally, the initiation species are formed from the hydrogen abstractions of the monomer by the radical cation of the dye and from the subsequent oxidations of the carbon-centered radicals of the monomer. Generally, photobleaching of the naphthoylenebenzimidazolone dyes also results from the further reduction of their protonated form.

1. Introduction

Photoinitiated free radical and cationic polymerizations have been the basis of numerous conventional applications, such as coatings, adhesives, inks, printing plates and microelectronics [1]. In contrast to thermal curing, photopolymerization can be performed at ambient temperature with solvent-free formulation, i.e., volatile organic compounds are not utilized. The great interest in light-induced cationic photopolymerization results from its several advantages over the corresponding free radical mode. For instance, this method may be used to polymerize important classes of monomers, e.g., epoxides and vinyl ethers [2,3], which have low volatilities and negligible toxicities. This method also has low shrinkage, high mechanical performance and good adhesion [2,3]. Additionally, cationic photopolymerization is not inhibited by oxygen, and photocuring can be performed in the presence of air. Lastly, the cationic cure of epoxide exhibits a dark-curing behavior, which is a particularly attractive property for materials used for the encapsulation of electronic devices [4,5].

Cationic photopolymerization is generally initiated by a Brönsted acid (H^+), which is formed during the photolysis of appropriate initiators. Various compounds have been synthesized and applied as sources of H^+ [3]. Among them, diaryliodonium salts are the most important because of their thermal stability, solubility in most cationic polymerized monomers, and their efficiencies in generating cationic species during irradiation. During UV irradiation, these salts undergo an irreversible photofragmentation, as shown in Scheme 1 for the diphenyliodonium compounds, and then the aryliodine radical cations or aryl cation generated further react with the solvent molecules or monomers to generate strong protic acids (H^+). These acids initiate the polymerizations of the monomers [3].

The development of efficient visible light emission sources, such as lasers and LEDs, for imaging, printing and medical applications has increased the demand for an initiator system that is effective in the 400–500 nm spectral region. Moreover, with exterior, durable photopolymers, the key has been to develop photoinitiators that will absorb outside of the UV absorption curve of traditional UV absorbers because that will protect the organic coatings from harmful Sun rays.

Unfortunately, iodonium salts absorb light below 300 nm, making them ineffective for the application where long-wavelength UV and visible light emission sources are used.

---

* Corresponding author. Tel.: +48 42 631 32 37; fax: +48 42 636 25 96.
E-mail addresses: radoslaw.podsiadly@p.lodz.pl, radekpod@p.lodz.pl (R. Podsiadły).

0143-7208/$ – see front matter © 2012 Elsevier Ltd. All rights reserved.
doi:10.1016/j.dyepig.2012.04.004

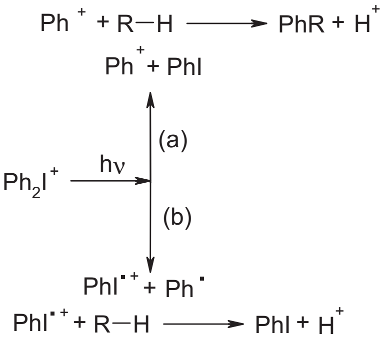

Scheme 1. Acid generation during the UV irradiation of iodonium salts. Heterolytic (a) and homolytic (b) Ph–I bond rupture.

Therefore, in the past decade, many efforts have been vested in the designs of visible light-sensitive onium salts [6–11,13–23], and there are two major strategies that enable to extend the spectral sensitivity of these salts. The first strategy is free radical promoted photosensitization (Scheme 2), in which radicals ($R^•$) are first generated from suitable systems (cleavage type or hydrogen abstraction type photoinitiators) and then oxidized by diaryliodonium salts [6–11], and the resulting cations initiate the polymerization. The drawback of this strategy is that oxygen inhibition will affect the radicals, as they will convert to peroxyl radicals ($ROO^•$) [12] and will become more difficult to oxidize [11].

The second employed strategy is the application of suitable sensitizers, which, after excitation, can react with onium salts via an electron transfer process, as illustrated in Scheme 3 for diphenyliodonium hexafluoroantimonate. In this strategy, the photoexcited sensitizer (Dye*) is oxidized by the onium salt ($Ph_2I^+SbF_6^-$) to form the corresponding radical cation ($Dye^{•+}$) and onium salt radical ($Ph_2I^•$). Due to the instability of the onium salt radical, its rapid decomposition retards any reverse electron transfers and renders the overall process irreversible. However, this mechanism also forms several cationic species, which can also initiate the polymerization: the radical cation ($Dye^{•+}$), which can initiate cationic polymerizations; the strong protic acid formed from the reaction between the $Dye^{•+}$ and solvent or monomer; and the carbocation of the monomer (M^+), which is formed during the oxidation of the monomer radical ($M^•$) by the iodonium salt [13].

Because the choices for an efficient visible sensitizer are rather limited for iodonium salt [14–17], the syntheses of new photosensitizers have received considerable attention [9,10,18–24]. Therefore, the main goal of this study was to apply naphthoylenebenzimidazolone dyes **1**–**5** as visible photosensitizers. These dyes were combined with commercially available onium salts, such as diphenyliodonium hexafluorophosphate (**On1**) and Irgacure 250 (**On2**), to create visible photoinitiating systems for the cationic polymerization of cyclohexene oxide (CHO). Iodonium salts were used as co-initiators (oxidizing agent). The structures of the studied dyes are presented in Scheme 4, and the structures of the iodonium salts are presented in Scheme 5. All of the co-initiators were applied as hexafluorophosphate salts. Additionally, this paper reports the photobleaching results of the studied dyes. Lastly, the detailed mechanism of the photochemical behavior of dye **1** was supported by the spectroscopic characterization of its radical cation $\mathbf{1}^{•+}$ and DFT calculation.

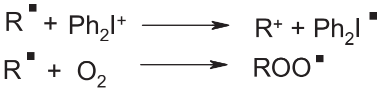

Scheme 2. Oxygen inhibition of the free radical.

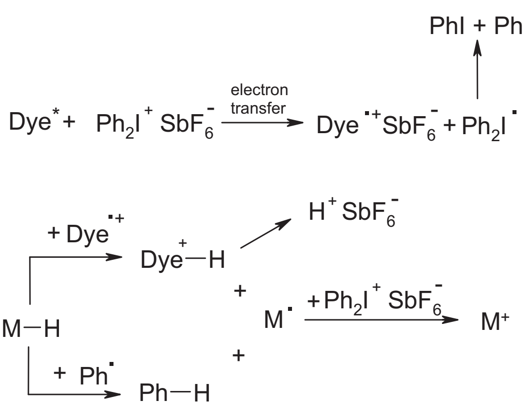

Scheme 3. Photooxidizable sensitization.

2. Experimental

2.1. General

The synthesis of each dye was performed as previously described [25]. The ionic liquid, 1-butyl-3-methylimidazolium hexafluorophosphate ($BMIM^+PF_6^-$), was prepared by the following method performed by Huddleston et al. [26]. The **On2** (Irgacure 250) salt was obtained from CIBA (Lodz, Poland), and **On1**, cyclohexene oxide (CHO), acetonitrile and methanol were purchased from Sigma–Aldrich (Poznan, Poland). All of the solvents were refluxed over CaH_2 and freshly distilled before use.

Absorption and steady state fluorescence spectra were recorded using a Jasco V 670 spectrophotometer and Jasco FP 6300 spectrofluorimeter (Jasco, Japan), respectively. All of the photochemical experiments were performed in a Rayonet Reactor RPR-200 (The Southern New England Ultraviolet Co., USA) equipped with lamps emitting light at 419 nm. A specific spectral band was isolated using band-pass filters at 419 ± 10 nm, and illumination intensities were measured using uranyl oxalate actinometry [27].

Singlet quenching constants were obtained from fluorescence quenching experiments, and the fluorescence spectra of the solutions of the dyes (6–14 μM) in CH_3CN, which contained various amounts of different quenchers, were measured at room temperature in the air by excitation at λ_{max}. The relative fluorescence intensities (I_0/I) were determined by measuring the heights of the peaks at λ_{em}.

2.2. Photochemical experiments

CHO (5 mL) was polymerized by radiation exposure for a specific time, and the resulting solution was poured into 50 mL of methanol containing approximately 1 mL of NH_3 (30%). The precipitated polymer was isolated by filtration, washed with cold methanol and dried overnight in a vacuum oven at 45 °C. The conversion of the

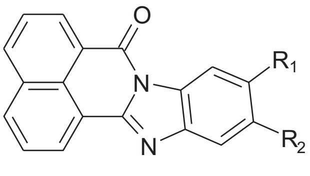

	R_1	R_2
1	H	H
2	Cl	H
3	Cl	Cl
4	Br	H
5	CH_3	CH_3

Scheme 4. Studied naphthoylenebenzimidazolone dyes.

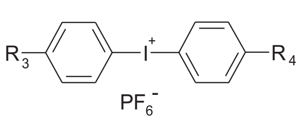

	R$_3$	R$_4$
On1	H	H
On2	CH$_3$	i-Pr

Scheme 5. Iodonium salts.

monomer into polymer was determined gravimetrically and calculated according to the Eq. (1):

$$\text{Conv. } (\%) = \frac{W_p}{W_m} \cdot 100\% \qquad (1)$$

where W_p and W_m are the weight of the polymer and the weight of the monomer, respectively.

The CHO conversion was calculated from at least three determinations. All of the photopolymerizations were conducted using a light wavelength of 419 nm and an irradiation intensity of 1.6×10^{17} quant s^{-1}. The concentrations of the dye and onium salt were 0.5 mM and 50.0 mM, respectively.

The photochemical reactions of the dyes with iodonium salt in CHO were performed in a glass tube under an air atmosphere. The extent of dye fading was determined based on the decrease in absorption at λ_{max}, and the quantum yield of the dye bleaching (Φ_{bl}) was calculated from at least three determinations when the reaction was 15 ± 2% complete.

2.3. Pulse radiolysis

Pulse radiolysis experiments were performed with high energy (6 MeV) 17 ns electron pulses generated from an ELU-6 linear electron accelerator. All of the measurements were performed at room temperature, and the dose absorbed per pulse was determined with a N_2O-saturated aqueous solution of KSCN (0.01 M), assuming $G((SCN)_2^{\bullet-}) = 6.2 \times 10^{-7}$ mol/J and $\varepsilon((SCN)_2^{\bullet-}) = 7600$ M^{-1} cm^{-1} (G represents the radiation chemical yield and ε is the molar absorption coefficient at 475 nm). The dose delivered per pulse was within the range of 5–80 Gy. Details of the pulse radiolysis system are provided elsewhere [28,29].

2.4. Radiolysis – cryogenic measurements

Glassy samples were prepared by quench-freezing the room temperature solutions in liquid nitrogen. The sample vial walls were 1–1.5 mm thick and were placed in a temperature-controlled, liquid nitrogen-cooled cryostat (Oxford Instruments, OptiStat DN). The desired temperature (77–150 K) of the matrix was attained by controlled automatic heating, and the samples mounted in the cryostat were irradiated with 4 μs electron pulses from the ELU-6 linear accelerator.

Radiolysis of the glassy sample of $BMIM^+PF_6^-$ and $CHCl_3$ led to the production of solvated electrons and oxidizing holes represented by the radical dication $BMIM^{2+\bullet}$ and $PF_6^\bullet$ (reaction 2) or the radical cation $CHCl_3^{\bullet+}$ (reaction 3). The addition of chloroform to the matrix not only improved the solubilities of many of the precursors but also improved the scavenging abilities of the electrons by the dissociative electron attachment (reaction 4), which led to a higher yield for the radical cations generated by radiolysis. The positive charge generated was transferred to the solute molecule with the lowest ionization potential (in this case, the dye) to give the corresponding radical cation (reactions 5–7).

$$BMIM^+, PF_6^- \rightarrow BMIM^{2+\bullet}, PF_6^\bullet, e^- \qquad (2)$$

$$CHCl_3 \rightarrow CHCl_3^{\bullet+} + e^- \qquad (3)$$

$$CHCl_3 + e^- \rightarrow CHCl_2^\bullet + Cl^- \qquad (4)$$

$$CHCl_3^{\bullet+} + \mathbf{1} \rightarrow CHCl_3 + \mathbf{1}^{\bullet+} \qquad (5)$$

$$BMIM^{2+\bullet} + \mathbf{1} \rightarrow BMIM^+ + \mathbf{1}^{\bullet+} \qquad (6)$$

$$PF_6^\bullet + \mathbf{1} \rightarrow PF_6^- + \mathbf{1}^{\bullet+} \qquad (7)$$

Additionally, upon the thermal annealing of the glassy samples, the chloromethyl radicals had already reacted with O_2; therefore, they formed the oxidizing peroxyl radicals (reaction 8) and subsequently oxidized dye **1** (reaction 9).

$$CHCl_2^\bullet + O_2 \rightarrow CHCl_2O_2^\bullet \qquad (8)$$

$$CHCl_2O_2^\bullet + \mathbf{1} \rightarrow CHCl_2O_2^- + \mathbf{1}^{\bullet+} \qquad (9)$$

2.5. Quantum chemical calculations

The geometries of all of the species were optimized by the B3LYP density functional method [30,31] as implemented in the Gaussian 03 suite of programs [32], and the optimized structures were characterized as local minima by a harmonic frequency analysis (all frequencies were real). For the ground state calculations, a standard 6-31G(d) basis set was utilized. The calculations for electronic excited states of the molecule were performed by the time-dependent DFT (TD-DFT) method [33] using the B3LYP functional method with the same basis set.

3. Results and discussion

3.1. Spectroscopic and thermodynamic properties of the naphthoylenebenzimidazolone dye/iodonium salt systems

Iodonium salts are among the main class of photoinitiators for cationic polymerizations. Unfortunately, these compounds have absorption bands in the UV region and are efficient photoinitiators of cationic polymerizations when irradiation is performed in the short- to mid-wavelength UV regions (230–300 nm). Therefore, to extend the spectral sensitivities to the visible light range, several photosensitizers that function via the oxidizable mechanism have been developed. For instance, dyes based on the naphthoylenebenzimidazolone skeleton have been applied as oxidizable sensitizers for free radical polymerizations [34]. Furthermore, high-efficiency free radical polymerizations initiated by photoredox pairs composed of dyes and N-alkoxypyridinium salts have been demonstrated and thus have encouraged us to apply naphthoylenebenzimidazolone dyes as photosensitizers for iodonium salts. In this study, the naphthoylenebenzimidazolone dyes (**1**–**5**) utilized have broad absorption bands at approximately 390 nm and each can be applied as a visible sensitizer for the collection of light at >400 nm; their spectroscopic and electrochemical properties are presented in Table 1. In such dye-based photoinitiator

Table 1
Spectroscopic and electrochemical properties of dyes **1**–**5**.

	λ_{max} [a], nm	τ_s [b], ns	$E_{ox}^{1/2}$ [c], V	E_{00} [d], eV	$\Phi(^1O_2)$ [d]
1	383	9.09	0.62	2.883	0.14
2	384	6.00	0.64	2.915	0.14
3	382	9.25	0.67	2.946	0.16
4	385	5.34	0.66	2.825	0.68
5	397	5.49	0.61	2.747	0.15

[a] In CHO.
[b] In MP from Ref. [35].
[c] In CH_3CN from Ref. [34].
[d] In MP from Ref. [34].

Table 2
Thermodynamic parameters of the studied photoredox pairs.

	On1 [a]			**On2** [b]		
	ΔG_{el}, eV	K_{SV}, M^{-1}	$k_q \times 10^{10}$, M^{-1} s^{-1}	ΔG_{el}, eV	K_{SV}, M^{-1}	$k_q \times 10^{10}$, M^{-1} s^{-1}
1	−1.683	61.44	0.68	−1.625	64.01	0.70
2	−1.695	49.70	0.83	−1.635	39.32	0.65
3	−1.696	47.98	0.52	−1.636	46.25	0.50
4	−1.585	35.17	0.66	−1.525	36.84	0.69
5	−1.557	59.23	1.08	−1.497	61.16	1.11

[a] $E_{red} = -0.58$ V (vs. Fc/Fc$^+$); $E_{red} = -0.2$ V (vs. SCE) from Ref. [9].
[b] $E_{red} = -0.64$ V vs. Fc/Fc$^+$ from Ref. [22].

systems, the initiator cationic species are typically generated by photoinduced electron transfers (Scheme 3). Therefore, intermolecular electron transfers between the excited dyes and iodonium salts must be thermodynamically allowed if the free energies, ΔG_{et}, calculated from the Rehm–Weller equation (Eq. (10)) [36] are negative.

$$\Delta G_{et} = E_{ox}(S/S^{\bullet+}) - E_{red}(A^{\bullet-}/A) - E^{00}(S) - Z_1Z_2/\varepsilon r_{12} \qquad (10)$$

In our investigation, ΔG_{et} was calculated using the oxidation potential E_{ox} (S/S$^{\bullet+}$), the singlet excited state energy E^{00}(S) of the dye (Table 1) and the reduction potential E_{red} (A$^{\bullet-}$/A) of the onium salts (see the bottom of Table 2). The Coulombic energy coefficient ($Z_1Z_2/\varepsilon r_{12}$) was omitted in these calculations because a neutral radical of the onium compound was formed ($Z = 0$) in the electron transfer process. The calculated thermodynamic parameters listed in Table 2, indicated that all the tested dye/iodonium salt systems posses a favorable thermodynamic driving force ($-\Delta G_{et} > 1.4$ eV) upon exposure to light. These results mean that their photoelectron transfer processes easily occur through the excited state. Furthermore, based on these calculations, the photodecompositions of the onium salts caused by the studied dyes are likely initiated by photoinduced intermolecular electron transfers from the dyes to the onium compound.

To further confirm the above calculations, quenching experiments in CH_3CN were performed. Examples of the fluorescence spectra for dye **1** recorded in CH_3CN and containing various amounts of **On1** are presented in Fig. 1. From these spectra, it is evident that the fluorescence of the naphthoylenebenzimidazolone dye **1** was effectively quenched by **On1**. Moreover, the same effect was also observed for the other dyes and iodonium salts studied. The absence of any new peaks in the emission spectra excludes any exciplex formation. To calculate the bimolecular quenching constants k_q from Eq. (11), the fluorescence lifetimes of the dyes (τ_0) without any quenchers were used [31].

Table 3
Conversion (%) of CHO initiated by the studied photoredox pairs.

	On1		**On2**	
	Conv [a]	Conv [b]	Conv [c]	Conv [d]
1	25.6	25.8	17.8	18.0
2	19.6	20.0	15.9	16.4
3	12.2	12.5	12.8	13.3
4	14.6	15.6	14.8	15.5
5	31.1	31.5	37.7	37.9

Irradiation intensity – 1.6×10^{17} quant s^{-1}.
[a] After 15 min of irradiation in air.
[b] After 15 min of irradiation in N_2.
[c] After 30 min of irradiation in air.
[d] After 30 min of irradiation in N_2.

$$I_0/I = 1 + k_q\tau_0[\mathbf{On}] \qquad (11)$$

The calculated singlet quenching constants (k_q) are summarized in Table 2. These values are close to the diffusion-controlled limits ($k_q \approx 1 \times 10^9 - 1 \times 10^{10}$ M^{-1} s^{-1}). Dye **5** had the highest value for k_q but also had the lowest oxidation potential. This finding suggests that fluorescent quenching proceeds via an electron transfer.

3.2. Photosensitized cationic polymerization

The photosystems composed of naphthoylenebenzimidazolone dyes **1**–**5** and iodonium salt were examined as photoinitiators in the cationic polymerization of CHO. Preliminary experiments show that CHO did not polymerize at 419 nm if any one component of the photoinitiator system was missing. Furthermore, the conversion of the monomer into polymer was determined after a specific irradiation time (Table 3). Fig. 2 shows an example of the relationship between the conversion of CHO and the irradiation time. The data presented in Table 3 clearly indicate that the efficiency of the CHO polymerization depends on both the dye and onium salt used. The highest efficiency for the CHO cationic polymerization was obtained for diphenyliodonium salt **On1**, whereas the lowest

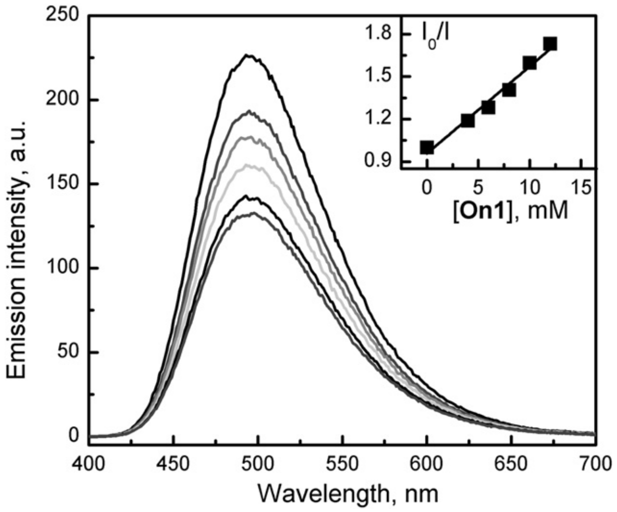

Fig. 1. Fluorescence quenching of dye **1** by **On1**. Inset: Stern–Volmer plot of fluorescence quenching of dye **1** (6 μM) by **On1** in CH_3CN.

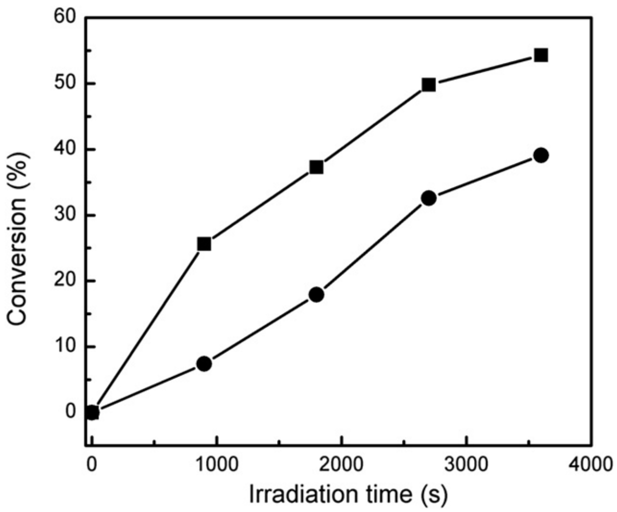

Fig. 2. Relationship between the cyclohexene oxide conversion and irradiation time. Dye **1** with **On1** (■) and **On2** (●).

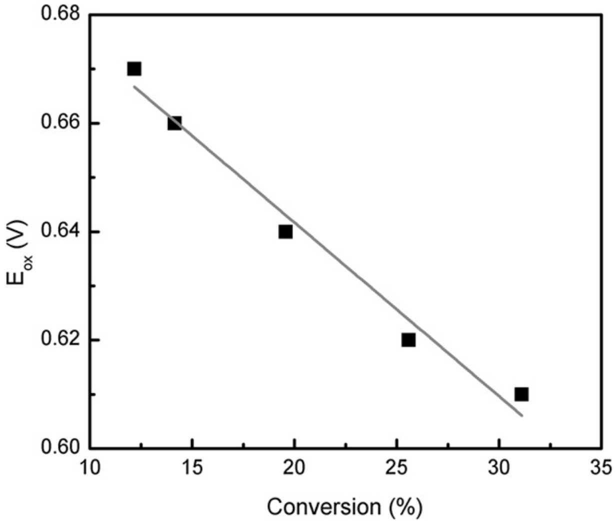

Fig. 3. Relationship between the conversion of cyclohexene oxide and the oxidation potentials of the dyes.

efficiency was obtained for **On2**. These results are related to different reduction potentials of the onium salts (see footnote of Table 2). Specifically, **On1** can be readily reduced in comparison with **On2** due to its lower reduction potential; therefore, the photoredox systems that contain **On1** have higher values for ΔG_{et} (Table 2). Moreover, it is evident from the data presented in Tables 1and 3 that the conversion of CHO depends on E_{ox} of the dye. This relationship is presented in Fig. 3.

For other iodonium-ketone systems, it has been suggested [13] that the triplet states of aromatic ketones, such as benzophenone, thioxanthones, benzil and quinones, react with H-donor compounds (monomers) to yield ketyl radicals, which oxidize back to sensitizers by the iodonium ions present, as shown in Scheme 6.

If such a mechanism works in the studied system, dyes with higher quantum yields for singlet oxygen generation [$\Phi(^1O_2)$] should have higher efficiencies for photopolymerization, especially under anaerobic conditions. From the data presented in Table 3, it is evident that dye **4** with the highest $\Phi(^1O_2)$ had the lowest conversion of CHO. Additionally, when the photopolymerization was performed in anaerobic conditions, the monomer conversion was imperceptibly higher in comparison with the CHO conversion in air atmosphere. Based on these results, one can exclude the participation of an excited triplet state in this photoreaction study. Moreover, as presented in Fig. 3, the linear relationship between the efficiencies of the CHO polymerizations and the E_{ox}s of the studied dyes suggests that the electron transfer from the dyes to the iodonium salts is the crucial step in these systems.

To understand this step further, the radical cation of dye **1** was characterized spectroscopically using the pulse radiolysis of low temperature matrices and the photochemical reaction of dye **1** with **On1** was studied in detailed.

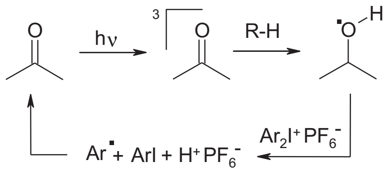

Scheme 6. Hydrogen abstraction via the ketone triplet state and oxidation of the ketyl radical.

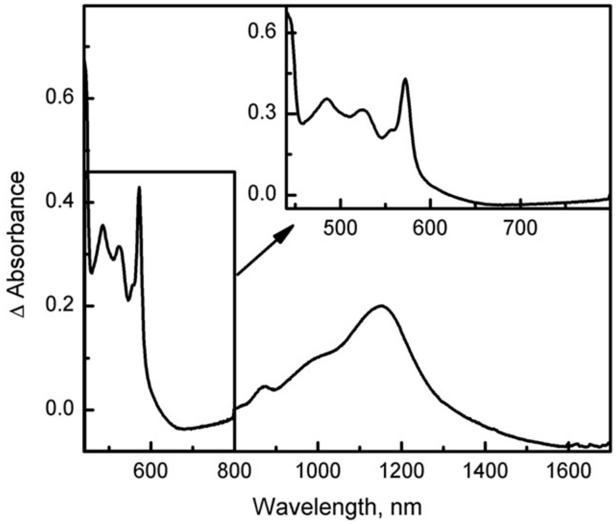

Fig. 4. Electronic absorption spectra obtained during the oxidation of **1** (c = 0.01 M) when embedded in a $BMIM^+PF_6^-$:$CHCl_3$ (1:1) matrix. The spectrum was collected after radiolysis at 77 K. The sample was 2-mm thick and received a radiation dose of 2.6 kGy.

*3.3. Photobleaching of dye **1** and the initiation mechanism*

In some papers that discuss photoinitiated cationic polymerizations, it has been suggested that after the electron transfer, stable radical cations of the sensitizers are formed [21,22,37,38]. Therefore, to confirm this theory, the pulse radiolysis of low temperature matrices was applied to spectroscopically characterize $\mathbf{1}^{\bullet+}$; the electronic absorption spectrum of the radical cation $\mathbf{1}^{\bullet+}$ is presented in Fig. 4. In the spectrum, a strong absorption band at 572 nm, two smaller peaks at shorter wavelengths 484 nm and 524 nm, and broad peaks at longer wavelengths starting at above 900 nm were present.

Knowing the absorption spectrum of $\mathbf{1}^{\bullet+}$, the photobleachings of the naphthoylene-benzimidazolone dyes with diphenyliodonium hexafluorophosphate were studied. The calculated photobleaching quantum yields are presented in Table 4, and an example of the absorption spectra of the combination of dye **1** and **On1** before and during irradiation in CHO are shown in Fig. 5.

During photolysis, decay of the dye absorption band at 383 nm was observed. Additionally, after 300 s of irradiation, new absorption bands at 378 nm and 395 nm were formed and a broad shoulder was observed at ~460 nm. Based on the absorption spectra in Figs. 4 and 5, one can conclude that radical cation $\mathbf{1}^{\bullet+}$ undergoes various subsequent reactions, and therefore $\mathbf{1}^{\bullet+}$ was not observed during steady state photolysis. However, it is also known in photopolymerizations that monomers, e.g., CHO, play the role of hydrogen donor [13]. Therefore, radical cation $\mathbf{1}^{\bullet+}$ could abstract hydrogen from CHO to form cations **6** or **7** (Scheme 7).

Table 4
Photobleaching quantum yields of the dyes (mmol quant^{-1}) with the iodonium salts in CHO.

	Φ_{bl} [a]	
	On1	**On2**
1	0.54	0.14
2	0.40	0.11
3	0.26	0.04
4	0.47	0.11
5	0.56	0.19

[a] Calculated for a 15 ± 2% dye conversion in air; irradiation intensity – 1.6×10^{17} quant s^{-1}.

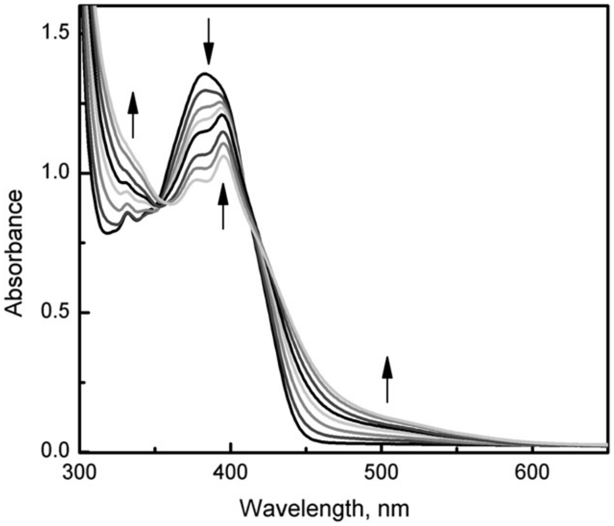

Fig. 5. Electronic absorption spectra obtained upon photolysis of the dye **1** (0.12 mM)/**On1** (10 mM) system in CHO under an air atmosphere (time interval – 60 s; irradiation intensity – 1.6×10^{17} quant s^{-1}).

In route a), $\mathbf{1}^{\bullet+}$ reacts with CHO via a hydrogen abstraction and then it donates a proton to regenerate dye **1**. In a study of the cationic polymerization of THF initiated by thioxantone and triarylsulfonium salt, this similar mechanism of acid release was also proposed as a crucial step in the reaction mechanism [38]. However, this mechanism did not explain the bleaching capabilities of the dye in the composition. For the second reaction route, formation of cation **7** via route b) is suggested to occur. DFT calculations at the B3LYP/6-31G(d) level were performed to compare the relative stabilities of cations **6** and **7**. Considering the high relative energy (95.7 kJ mol^{-1}) of cation **6** relative to cation **7**, one can assume that radical cation $\mathbf{1}^{\bullet+}$ reacts with hydrogen at the imidazole nitrogen. Moreover, TD-DFT calculation at the B3LYP/6-31G(d) level reveals that cation **7** shows an absorption band in the same wavelength as the product formed during photolysis (Table 5).

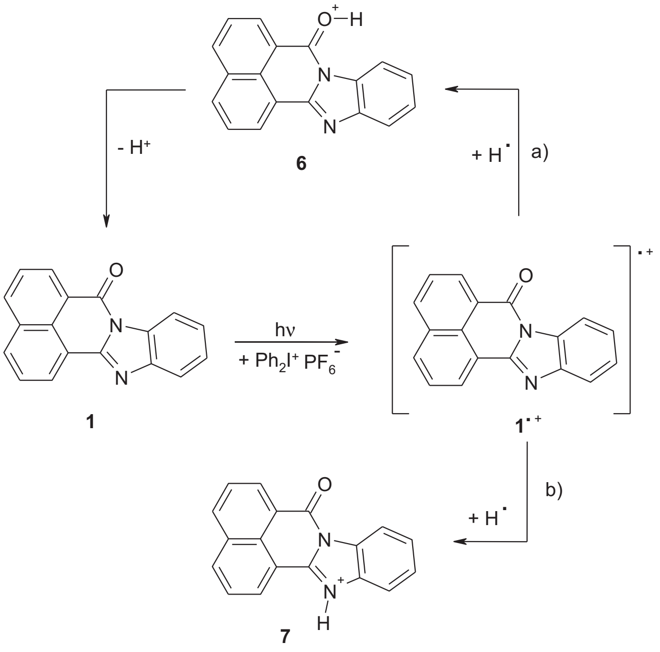

Scheme 7. Possible reactions for radical cation $\mathbf{1}^{\bullet+}$.

Table 5
Comparison of experimental absorption maxima recorded during photolysis of **1**/**On1** and calculated absorption maxima of cations **6** and **7**.

	Wavelength, nm (oscillator strength)
1/On1	396, 379
6	601.02 (0.0620); 455.76 (0.1507); 368.17 (0.0427); 353.18 (0.0588); 339.17 (0.0003); 298.90 (0.3675); 276.37 (0.0526); 273.19 (0.0020); 263.28 (0.0810); 252.35 (0.4213).
7	396.73 (0.3712); 372.07 (0.0103); 338.68 (0.0197); 326.14 (0.0556); 281.12 (0.0739); 253.10 (0.0134); 249.47 (0.1083); 242.46 (0.0936); 238.83 (0.1020).

To confirm this calculation, the photolysis of **1**/**On1** in CHO with a proton scavenger was performed. From Table 6, the addition of 2,6-di-tert-butyl-4-methylpyridine (TBP) did not noticeably influence the Φ_{bl} of **1** or the formation of **7**. Moreover, TBP did not inhibit the polymerization of CHO. Therefore, the formation of the Brønsted acid via route a) was excluded.

To further confirm the formation of cation **7** during photolysis, the spectra of dye **1** recorded at different pHs in 2-PrOH (Fig. 6) were taken. From these spectra, increasing the pH value diminished of the UV absorption bands at 283 nm and 294 nm and increased the band at 394 nm. This same absorption band was observed during the irradiation of the **1**/**On1** photoredox pairs in CHO (Fig. 5 and Table 6).

The formation of this cation has several consequences. For instance, considering the reduction potentials of the neutral species **1** and cationic dye **8** (Scheme 8) ($E_{1/2} = -1.62$ V and $E_{1/2} = -1.02$ V, respectively [25]), one can assume in the presence of an electron donor or hydrogen donor that the cationic species should undergo a further photochemical reduction. To confirm this suggestion, the irradiation of cationic naphthoylenebenzimidazolone dye **8** in CHO was performed. The calculated Φ_{bl} for this dye is presented in Table 6, whereas the recorded absorption spectra before and during irradiation are shown in Fig. 7. From these data, decay of the dye absorptions at 391 nm and 409 nm was accompanied by the growth of the band at 373 nm and two small bands at ~465 nm and ~495 nm. Therefore, one can conclude that the reduction of cation **7** caused the final bleaching of dye **1**. Moreover, polymer was not formed when the photolysis was performed without **On1** (Table 6).

These findings suggest that the photoreductions of the naphthoylenebenzimidazolone dyes occur via hydrogen abstractions.

Table 6
Absorption bands (λ, nm), photobleaching quantum yields (Φ_{bl}, mmol quant^{-1}) and CHO conversions (%) observed during photolyses of dyes **1** and **8** in different conditions.

Dye [a]	Additive	Solvent/Monomer	λ, nm (Φ_{bl}, mmol quant^{-1})	Conversion [g]
1	None	CHO [d]	No change	No polymer
1	**On1** [b]	CHO [d]	379, 396 (0.48 [f])	7%
1	**On1** [b]	CHO [e]	379, 396 (0.69 [f])	6%
1	**On1** [b]/**TBP** [c]	CHO [d]	379, 396 (0.47 [f])	6%
1	None	2-PrOH [d]	No change	–
1	HCl (pH = 0.18)	2-PrOH [d]	394	–
8	None	CHO/MeCN [d]	373 (28.7 [f])	No polymer
8	**On1** [b]	CHO/MeCN [d]	391 (0.35 [f])	3%

[a] [dye] = 0.1 mM.
[b] [**On1**] = 10 mM.
[c] [TBP] = 10 mM.
[d] In air; irradiation intensity – 8.0×10^{16} quant s^{-1}.
[e] Under N_2; irradiation intensity – 8.0×10^{16} quant s^{-1}.
[f] Calculated for a 9 ± 2% dye conversion.
[g] After 10 min of irradiation; irradiation intensity – 8.0×10^{16}.

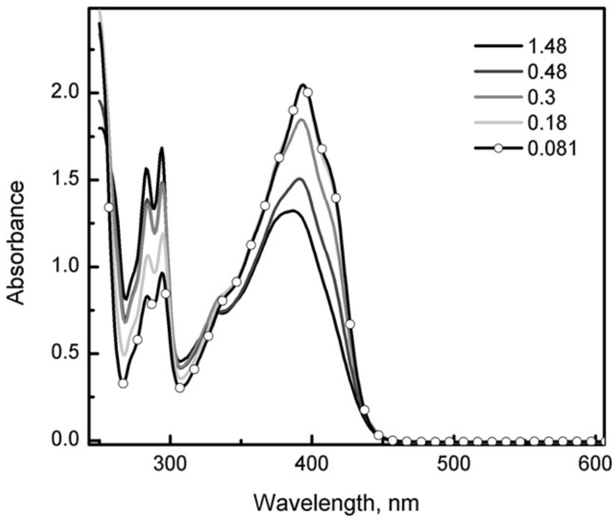

Fig. 6. Electronic absorption spectra of dye **1** (0.1 mM) in 2-PrOH for different pHs.

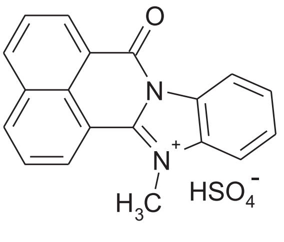

8

Scheme 8. Structure of cationic dye **8**.

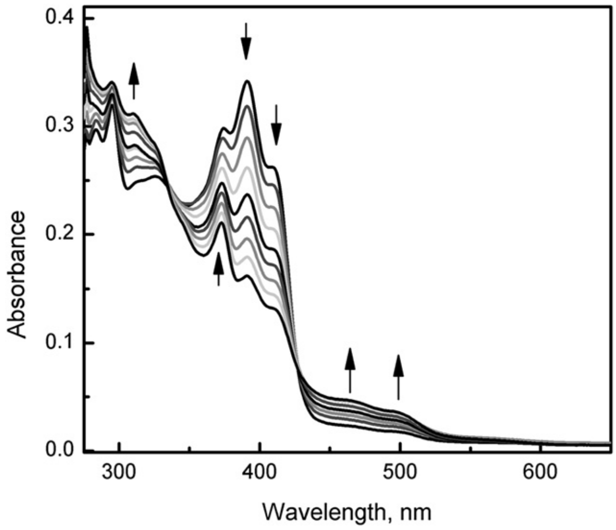

Fig. 7. Electronic absorption spectra obtained upon photolysis of dye **8** (0.17 μM) in CHO under an air atmosphere (time interval – 30 s; irradiation intensity – 1.4×10^{17} quant s^{-1}).

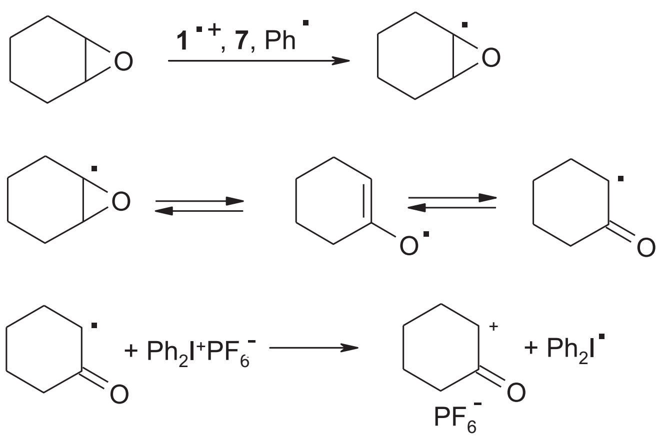

Scheme 9. Photochemical generation of the carbocation of CHO.

Furthermore, the abstraction of the epoxide hydrogen by $\mathbf{1}^{\bullet+}$, **7** or $Ph^{\bullet}$ (Scheme 9) results in carbon-centered CHO radicals, which should form readily because the radicals can stabilize by resonance. However, the monomer radical can also be oxidized by the diaryliodonium salt to yield a carbocation. In a subsequent step, diaryliodone radical can undergo an irreversible fragmentation to form iodoaromatic compounds and an aryl radical. This aryl radical can also abstract a hydrogen atom from the monomer [13].

4. Conclusions

Naphthoylenebenzimidazolone dyes, when combined with commercially available onium salts, such as diphenyliodonium hexafluorophosphate (**On1**) and Irgacure 250 (**On2**), have the ability to be used with practical applications as visible light photoinitiators of cationic polymerizations. The ability of a photoredox pair to act as a photoinitiator strongly depends upon the E_{ox} of the dye and E_{red} of the iodonium salt. Furthermore, the initiator species formed are the results of the hydrogen abstractions by the cation radicals of the dye and monomer and of the subsequent oxidations of the carbon-centered monomer radical. Finally, photobleaching of the naphthoylenebenzimidazolone dyes is a result of the further reduction of their protonated forms.

References

[1] Yagci Y, Jockusch S, Turro NJ. Photoinitiated polymerization: advances, challenges, and opportunities. Macromolecules 2010;43:6245–60.
[2] Fouassier JP, Rabek J. Radiation curing in polymer science and technology. London: Elsevier; 1993. pp. 49–113.
[3] Schnabel W. Polymers and light: fundamentals and technical application. Weinheim: Wiley-VCH; 2007. pp. 275–329.
[4] Voytekunas VY, Ng FL, Abadie MJM. Kinetics study of the UV initiated cationic polymerization of cycloaliphatic diepoxide resins. Eur Polym J 2008;44:3640–9.
[5] Jung-Dae C, Jin-Who H. Photo-curing kinetics for the UV-initiated cationic polymerization of a cycloaliphatic diepoxide system photosensitized by thioxanthone. Eur Polym J 2005;41:367–74.
[6] Durmaz YY, Moszner N, Yagci Y. Visible light initiated free radical promoted cationic polymerization using acylgermane based photoinitiator in the presence of onium salts. Macromolecules 2008;41:6714–8.
[7] Crivello JV. A new visible light sensitive photoinitiator system for the cationic polymerization of epoxides. J Polym Sci Part A Polym Chem 2009;47:866–75.
[8] Lalevée J, Dirani A, El-Roz M, Allonas X, Fouassier JP. Germanes as efficient coinitiators in radical and cationic photopolymerizations. J Polym Sci Part A Polym Chem 2008;46:3042–7.
[9] Yilmaz G, Beyazit S, Yagci Y. Visible light induced free radical promoted cationic polymerization using thioxanthone derivatives. J Polym Sci Part A Polym Chem 2011;49:1591–6.
[10] Tunc D, Yagci Y. Thioxanthone-ethylcarbazole as a soluble visible light photoinitiator for free radical and free radical promoted cationic polymerizations. Polym Chem 2011;2:2557–63.
[11] Lalevée J, El-Roz M, Allonas X, Fouassier JP. Free-radical-promoted cationic photopolymerization under visible light in aerated media: new and highly efficient silane-containing initiating systems. J Polym Sci Part A Polym Chem 2008;46:2008–14.

[12] Maillard B, Ingold KU, Scaiano JC. Rate constants for the reactions of free radicals with oxygen in solution. J Am Chem Soc 1983;105:5095–9.

[13] Crivello JV, Sangermano M. Visible and long-wavelength photoinitiated cationic polymerization. J Polym Sci Part A Polym Chem 2001;39: 343–56.

[14] Zhu QQ, Schnabel W. Cationic photopolymerization under visible laser light: polymerization of oxiranes with coumarin/onium salt initiator systems. Polymer 1996;37:4129–33.

[15] Selvaraju C, Sivakumar A, Ramamurthy P. Excited state reactions of acridinedione dyes with onium salts: mechanistic details. J Photochem Photobiol A Chem 2001;138:213–26.

[16] Neumann MG, Rodriques MR. A study of the elemental reactions involved in the initiation of the polymerization of tetrahydrofuran induced by the photosensitization of a triphenylsulphonium salt by perylene. J Braz Chem Soc 2003;14:76–82.

[17] Crivello JV, Bulut U. Curcumin: a naturally occurring long-wavelength photosensitizer for diaryliodonium salts. J Polym Sci Part A Polym Chem 2005;43:5217–31.

[18] Aydogan B, Gundogan AS, Ozturk T, Yagci Y. A dithienothiophene derivative as a long-wavelength photosensitizer for onium salt photoinitiated cationic polymerization. Macromolecules 2008;41:3468–71.

[19] Tasdelen MA, Kumbaraci V, Jockusch S, Turro NJ, Talinli N, Yagci Y. Photoacid generation by stepwise two-photon absorption: photoinitiated cationic polymerization of cyclohexene oxide by using benzodioxinone in the presence of iodonium salt. Macromolecules 2008;41:295–7.

[20] Podsiadły R. The synthesis of novel, visible-wavelength oxidizable polymerization sensitizers based on the 5,12-dihydroquinoxalino[2,3-b]pyridopyrazine skeleton. Dyes Pigm 2009;80:86–92.

[21] Podsiadły R. 12H-quinoxalino[2,3-b][1,4]benzothiazine derivatives as novel visible photosensitizers in cationic photopolymerization. J Photochem Photobiol A Chem 2009;208:147–53.

[22] Narewska J, Strzelczyk R, Podsiadły R. Fluoflavin dyes as electron transfer photosensitizers for onium salt induced cationic photopolymerization. J Photochem Photobiol A Chem 2010;212:68–74.

[23] Bulut U, Gunbas GE, Toppare L. A quinoxaline derivative as a long wavelength photosensitizer for diaryliodonium salts. J Polym Sci Part A Polym Chem 2010; 48:209–13.

[24] Bulut U, Balan A, Calaskin C. Benzotriazole derivatives as long wavelength photosensitizers for diaryliodonium salt initiators. J Polym Sci Part A Polym Chem 2011;49:729–33.

[25] Podsiadły R, Kolińska J, Sokołowska J. Study of free radical polymerisation with dye photoinitiators containing a naphthoylenebenzimidazolone skeleton. Coloration Technol 2008;124:79–85.

[26] Huddleston JG, Willauer HD, Swatlowski RP, Visser AE, Rogers RD. Room temperature ionic liquids as novel media for ‘clean’ liquid–liquid extraction. Chem Commun 1998;16:1765–6.

[27] Leighton WB, Forbes GS. Precision actinometry with uranyl oxalate. J Am Chem Soc 1930;52:3139–52.

[28] Karolczak S, Hodyr K, Łubis R, Kroh J. Pulse radiolysis system based on ELU-6E LINAC. J Radioanal Nucl Chem 1986;101:177–88.

[29] Karolczak S, Hodyr K, Połowiński M. Pulse radiolysis system based on ELU-6E Linac II. Development and upgrading the system. Radiat Phys Chem 1992;39:1–5.

[30] Becke AD. Density-functional thermochemistry. III. The role of exact exchange. J Chem Phys 1993;98:5648–52.

[31] Lee C, Yang W, Parr RG. Development of the Colle-Salvetti correlation-energy formula into a functional of the electron density. Phys Rev B 1988;37:785–9.

[32] Gaussian 03, revision B.01. Pittsburgh PA: Gaussian, Inc.; 2003.

[33] Bauernschmitt R, Ahlrichs R. Treatment of electronic excitations within the adiabatic approximation of time dependent density functional theory. Chem Phys Lett 1996;256:454–64.

[34] Kolińska J, Podsiadły R, Sokołowska J. Naphthoylenebenzimidazolone sensitisers for photo-oxidisable free radical polymerisation with the aid of pyridinium salts. Coloration Technol 2008;124:341–7.

[35] Kolińska J, Podsiadły R, Wysocki S, Sokołowska J. The photochemical behavior of naphthoylenebenzimidazolone dyes in 1-methyl-2-pyrrolidone. Dyes Pigm 2009;82:238–43.

[36] Rehm D, Weller A. Kinetics of fluorescence quenching by electron and H-atom transfer. Isr J Chem 1970;8:259–71.

[37] Cook WD, Chen S, Chen F, Kahveci MU, Yagci Y. Photopolymerization of vinyl ether networks using an iodonium initiator – The role of photosensitizers. J Polym Sci Part A Polym Chem 2009;47:5474–87.

[38] Neumann MG, Rodriques MR. Mechanistic study of tetrahydrofuran polymerization photoinitiated by a sulfonium salt/thioxanthone system. Macromol Chem Phys 2001;202:2776–82.